DNA Binding to Crystalline Silica Characterized by Fourier-Transform Infrared Spectroscopy

Yan Mao,[1] Lambert N. Daniel,[1] Noel Whittaker,[2] and Umberto Saffiotti[1]

[1]Laboratory of Experimental Pathology, National Cancer Institute, National Institutes of Health, Bethesda, Maryland; [2]Laboratory of Analytical Chemistry, National Institute of Diabetes and Digestive and Kidney Diseases, National Institutes of Health, Bethesda, Maryland

The interaction of DNA with crystalline silica in buffered aqueous solutions at physiologic pH has been investigated by Fourier-transform infrared spectroscopy (FT-IR). In aqueous buffer, significant changes occur in the spectra of DNA and silica upon coincubation, suggesting that a DNA–silica complex forms as silica interacts with DNA. As compared to the spectrum of silica alone, the changes in the FT-IR spectrum of silica in the DNA–silica complex are consistent with an Si—O bond perturbation on the surface of the silica crystal. DNA remains in a B-form conformation in the DNA–silica complex. The most prominent changes in the DNA spectrum occur in the 1225 to 1000 cm^{-1} region. Upon binding, the PO_2^- asymmetric stretch at 1225 cm^{-1} is increased in intensity and slightly shifted to lower frequencies; the PO_2^- symmetric stretch at 1086 cm^{-1} is markedly increased in intensity; and the band at 1053 cm^{-1}, representing either the phosphodiester or the C—O stretch of DNA backbone, is significantly reduced in intensity. In D_2O buffer, the DNA spectrum reveals a marked increase in intensity of the peak at 1086 cm^{-1} and a progressive decrease in intensity of the peak at 1053 cm^{-1} when DNA is exposed to increasing concentrations of silica. The carbonyl band at 1688 cm^{-1} diminishes and shifts to slightly lower frequencies with increasing concentrations of silica. The present study demonstrates that crystalline silica binds to the phosphate-sugar backbone of DNA. The close proximity of the silica surface to the DNA molecule, brought about by this binding, may contribute to DNA strand breakage produced by silica-derived free radicals. The ability of silica to form stable complexes with DNA may play an important role in the mechanisms of silica-induced toxicity and carcinogenesis. — Environ Health Perspect 102(Suppl 10):165–171 (1994)

Key words: silica, DNA adducts, Fourier-transform infrared spectroscopy, silicosis, carcinogenesis

Introduction

The deposition of crystalline silica particles (hereafter referred to as silica) in the lung of humans or experimental animals leads to silicosis, a progressive pulmonary disease characterized by a fibrotic granulomatous reaction (*1*). Since the early 1980s, epidemiologic studies have reported the association of silicosis with an increased risk for lung cancer (*2–4*). Experimental treatment of rats with silica by inhalation or by intratracheal instillation induced high incidences of fibrosis-associated pulmonary carcinomas (*2,3,5–7*). In cell culture assays, silica has been shown to stimulate the proliferation of fibroblasts (*8*) and alveolar epithelial cells (*9,10*) and to induce neoplastic transformation (*11,12*).

It is generally believed that the surface reactivity of silica with cellular components is a key to understanding its mechanism of action. As proposed by Nash et al. (*13*), the nonionized silanol group on the hydrated silica surface is a hydrogen donor group, which can form hydrogen bonds with a hydrogen acceptor. For example:

$$\equiv Si\text{–}OH + O{=}N\text{–} \rightarrow \equiv Si\text{–}OH\cdots\cdots O{=}N\text{–}$$

$$\equiv Si\text{–}OH + O{=}P{\equiv} \rightarrow \equiv Si\text{-}OH\cdots\cdots O{=}P{\equiv}$$

$$\equiv Si\text{–}OH + NH{=} \rightarrow \equiv Si\text{–}OH\cdots\cdots NH{=}$$

This hypothesis, supported by the observation that silica can react with protein, phospholipids, and biologic membrane systems, has been considered by most investigators as a general model of interaction of silica with biologic macromolecules (*14,15*). However, silica has also recently been shown to generate free radicals detectable by electron spin resonance (ESR) spectroscopy under a variety of experimental conditions (*16–18*). It was proposed that these free radicals play an important role in the mechanism of silica toxicity and carcinogenicity (*19–23*).

The present study was initiated to further investigate the mechanisms by which silica can cause DNA strand breaks *in vitro* (*24*). The application of Fourier-transform infrared (FT-IR) absorption spectroscopy to the study of biomolecules in an aqueous environment has several advantages (*24,25*). High quality spectra of DNA and protein can be obtained with relative ease in aqueous solutions without associated background fluorescence, which is an overwhelming effect for the complementary vibrational technique of Raman spectroscopy (*25*). FT-IR spectroscopy can monitor absorption from all bonds of the biomolecules and does not rely on the use of additional probe molecules, as is required with some other spectroscopic methods. FT-IR spectroscopy has been successfully used to study DNA–peptide and DNA–drug interactions (*26–28*).

Materials and Methods

Silica Preparations

A sample of min-U-sil 5 α-quartz (MQZ, Pennsylvania Glass Sand Co., (Pittsburgh PA) was obtained through the Illinois Institute of Technology Research (Chicago, IL) and tested for biologic activity *in vivo* and *in vitro* (*5,6,12,21*). Chinese standard α-quartz (CSQZ), which is used as a standard sample in China (*29*), was obtained from Nanjing University (Nanjing, China). The purity of silica was >99% and the particle size was mostly between 0.5 and 3 μm in both samples. The median distribution by number was 1.1 to 2 μm and 0.5 to 1 μm for MQZ and CSQZ, respectively, and the surface areas (by nitrogen adsorption) (*30*) were 3.15 $mm^2/\mu g$ and 11.66 $mm^2/\mu g$ (*31*).

This paper was presented at the Conference on Oxygen Radicals and Lung Injury held 30 August–2 September 1993 in Morgantown, West Virginia.

The authors thank Dr. Ira W. Levin for his encouragement, suggestions, and criticisms.

Address correspondence to Lambert N. Daniel, Laboratory of Experimental Pathology, Division of Cancer Etiology, National Cancer Institute, Bethesda, MD 20892-0041. Telephone (301) 496-2818. Fax (301) 402-1829.

Silica samples were dried in an oven at 110°C for 24 hr before each experiment and then suspended in buffer at a concentration of 20 mg/ml. Homogeneous silica suspensions were obtained by sonication in a Branson model 220 cleaning sonicator (Shelton, CT) for 3 min. The suspensions were diluted to a desired concentration and used immediately.

Chemical modification of silica surfaces was performed using poly(2-vinylpyridine-*n*-oxide)(PVPNO)(Polysciences, Inc., Warrington, PA), which is known to bind to silanol groups on the silica surface (*32*). For each silica modification, 1.5 ml of a freshly suspended 10 mg/ml silica suspension was added to 1.5 ml of a 100 µg/ml PVPNO, 5 mM phosphate buffer solution, pH 7.4, in a 15 ml polystyrene tube and tightly capped. Following incubation at 37°C in a shaking incubator for 1 hr, samples were then divided into two 2-ml plastic tubes and centrifuged 30 min at 12,000 rpm in an Eppendorf microcentrifuge. The pellet was resuspended in 1.5 ml phosphate buffer.

DNA and Chemicals

λ-DNA was purchased from BRL (Gaithersburg, MD). Calf thymus DNA, AMP, CMP, GMP, TMP, sodium phosphate, and deuterium oxide (D_2O, 99.9%) were all obtained from Sigma (St. Louis, MO). Phosphate buffers were titrated to pH 7.4 at 25°C by mixing divalent and monovalent stock solutions and were treated with Chelex resin (BioRad, Richmond, CA). The buffer was diluted to 5 mM by H_2O or D_2O. The pH or pD of the buffers was 7.4. The pD of the phosphate buffer in D_2O was determined by adding 0.45 to the pH meter reading (*33*).

FT-IR Studies

Attenuated Total Reflectance Fourier-Transform Infrared (ATR FT-IR) Spectra. The ATR FT-IR spectroscopic techniques employed were based on previously published methods (*26*). A Digilab single-beam FTS-45 FT-IR spectrophotometer (BioRad, Cambridge, MA) was used to obtain spectra of the samples at ambient temperatures using a DTGS detector. The spectral resolution was 8 cm^{-1}. This spectral resolution has been shown to give optimal signal to noise ratios with reproducibly accurate band position assignments within less than 1 cm^{-1} (*26,27,34*). A triangular apodization was applied after recording 1000 scans for each sample. The samples were scanned in a Bio-Rad liquid ATR cell (part number 099-1031) with a ZnSe (45°) crystal. For such an arrangement, the total volume of sample used for one experiment was 1.8 ml. The cell and the crystal were thoroughly cleaned by washing with water and air-dried after each experiment. The spectral region scanned was between 2500 and 740 cm^{-1} for the H_2O solution and between 2000 and 740 cm^{-1} for the D_2O solution. Analysis of the spectra, however, was limited to the 1800 to 800 cm^{-1} range. All ATR spectra were recorded under a nitrogen atmosphere to eliminate water vapor interference. Spectra were obtained for the silica suspension alone (0.2, 1, and 5 mg/ml), calf thymus DNA alone (10 mg/ml), and a mixture (silica 0.2, 1, or 5 mg/ml, and DNA 10 mg/ml). Suspensions were mixed in 5 mM phosphate buffer at pH 7.4. The DNA was allowed to dissolve in 5 mM phosphate buffer for at least 24 hr to insure the formation of a homogeneous solution. Infrared absorbance by buffer components was not detectable and incubations in plain water gave similar results (data not shown). The samples were incubated for 15 hr at 37°C before measurement. Vibrational signals arising from buffer components were subtracted from all sample spectra using the Digilab software. The criteria (*35,36*) for water buffer subtraction were: absence of the H_2O association band at 2130 cm^{-1} (neither DNA nor silica absorb at this frequency, so this line is a suitable internal standard for water subtraction); presence of a flat baseline in the 2000 to 800 cm^{-1} range; and no negative lobes in the spectrum. The criterion for subtraction of D_2O buffer was to obtain a flat baseline in the 1900 to 1725 cm^{-1} region after the subtraction step.

To observe the effects of coincubation of silica with DNA on the respective spectra, the spectrum of each component was subtracted from the spectrum of the combination (DNA + silica). The peaks in the silica spectrum at 779 and 799 cm^{-1} identified by transmission IR (see below) are also seen using ATR in D_2O. These peaks were not affected by coincubation with DNA (data not shown) and therefore were used as an internal normalization standard for silica to obtain a correct silica subtraction from the combination (DNA + silica) spectra. The value of the subtraction factor (about 1.025) was selected when the D_2O band in the 1900 to 1725 cm^{-1} region became flat and the peaks at 779 and 799 cm^{-1} disappeared. The same subtraction factor for silica was used for (DNA + silica) combination in H_2O. The criterion for DNA subtraction was the presence of a flat baseline in the 1750 to 1200 cm^{-1} range.

Transmission FT-IR Spectra. For transmission FT-IR spectroscopy, 40 µl of a 5 mg/ml silica suspension was spread as a film on a ZnSe window and then exposed to vacuum to dry the sample before placing it in the infrared cell. Phosphate buffer was added in a variable amount to give a desired degree of hydration to the dry silica films. The transmission FT-IR spectrum for silica as a dried film was similar to previously published studies (*37*).

Results

Changes in DNA Spectra after Silica–DNA Coincubation

DNA Interaction with Silica in Buffered H_2O. Figure 1 demonstrates a typical ATR FT-IR spectrum of calf thymus DNA and the spectra of DNA coincubations with silica (minus a silica control). The control DNA spectrum (Figure 1*A*) is essentially identical with those reported by others (*24,26*), and the assignment of the bands in the spectrum is given in Table 1. Only the spectral interval range between 1800 and 900 cm^{-1} was examined.

Both tested quartz samples, MQZ and CSQZ, produced significant alterations of the DNA spectra. In comparison with the spectrum of DNA (Figure 1*A*), the carbonyl stretching modes at 1715 cm^{-1} in the spectrum of the DNA with either MQZ or CSQZ (Figure 1*B,C*) remained relatively constant, indicating that the B conformation of DNA persisted in the DNA–silica complex.

The intensities and frequencies of bands between 1715 and 1250 cm^{-1} changed only slightly with silica coincubation. By contrast, there were considerable changes in the 1250 to 900 cm^{-1} region. The peak corresponding to the phosphate asymmetric stretch in DNA shifted from 1225 cm^{-1} to 1223 and 1222 cm^{-1} for DNA + MQZ and DNA + CSQZ, respectively (Figure 1*A–C*). The intensities of these peaks increased as well. Moreover, the intensity of the peak corresponding to the phosphate symmetric stretching mode at 1086 cm^{-1} in DNA markedly increased in the DNA plus silica complex. The band at 1053 cm^{-1} was reduced in intensity and slightly shifted to a higher frequency. In addition, the relative intensities in the peaks at 1086 and 1053 cm^{-1} changed, and the ratio of the peaks increased markedly from 1.56 to 3.46.

The findings from the tests in H_2O indicate structural changes in the DNA

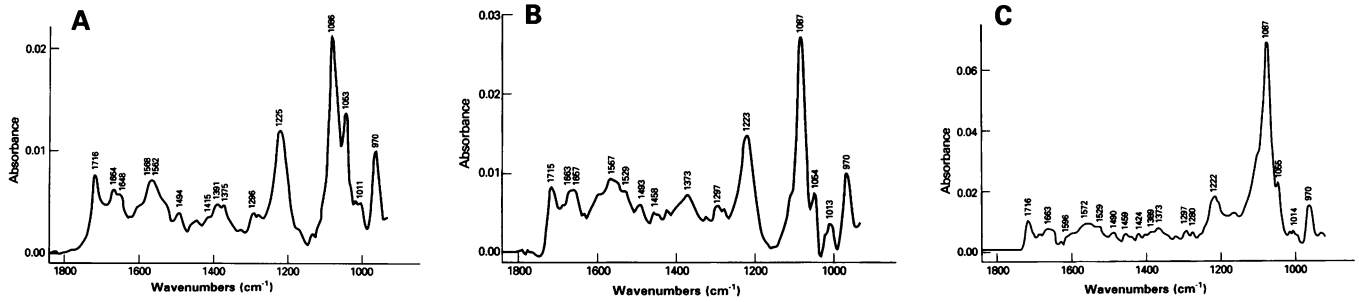

Figure 1. ATR FT-IR spectrum of calf thymus DNA (10 mg/ml in pH 7.4 phosphate-buffered H_2O) in the region 900–1800 cm^{-1} and the spectra of DNA coincubations with silica (5 mg/ml). Note different scales of Y axes. (*A*) DNA alone; (*B*) (DNA + MQZ)–MQZ (subtraction factor is 1.025); (*C*) (DNA + CSQZ) – CSQZ (subtraction factor is 1.030).

Table 1. Assignment of bands in FT-IR spectrum (1000–1800 cm^{-1}) of DNA (10 mg/ml) in buffered H_2O.

Wave number, cm^{-1}	Relative absorbance	Assignment[a]
1716	0.008	C=O of guanine
1664	0.006	C=C, C=N in the base planes
1648	0.006	C=C, C=N in the base planes
1568	0.007	C=C, C=N in the base planes
1562	0.007	C=C, C=N in the base planes
1494	0.005	Base–sugar moieties
1415	0.004	Base–sugar moieties
1391	0.005	Base–sugar moieties
1375	0.005	Base–sugar moieties
1296	0.005	Base–sugar moieties
1225	0.012	Asymmetric PO_2^- stretching
1086	0.021	Symmetric PO_2^- stretching
1053	0.014	P–O or C–O backbone stretch
1011	0.005	P–O or C–O backbone stretch

[a] From Taillandier and Liquier (*24*) and Dev and Walters (*26*).

backbone due to a reorientation of the phosphate groups and involvement of the phosphates in the interaction of DNA with silica.

DNA Interaction with Silica in Buffered D_2O. Water absorbance makes it difficult to obtain data in the regions around 1600 cm^{-1} and below 1000 cm^{-1}. These spectral regions reflect the vibrations of the C=O, C=C, and C=N linkages in the base planes and the vibrations of the phosphodiester moiety that is coupled to the sugar groups (*24*). By replacing H_2O with D_2O in 5 mM phosphate buffer, pD 7.4, the overlapping of solvent modes with the DNA spectral features was avoided.

The effect on the DNA spectrum from increasing amounts of silica was evident, namely, a marked increase in the intensity of the peak at 1086 cm^{-1} and a progressive loss of intensity at 1053 cm^{-1} (Figure 2). It was also evident from the spectra that silica perturbed the frequencies and intensities of modes corresponding to the sugar–phosphate linkage. The behaviors of the bands in the 1100 to 800 cm^{-1} are given in Table 2 for the DNA control and the mixtures of DNA + silica obtained in D_2O solution.

Smaller, but significant differences in the 1800 to 1500 cm^{-1} region were observed in D_2O buffer. The high frequency band at 1688 cm^{-1} in the DNA control became weaker and shifted to lower frequencies as the concentration of added silica increased (Figure 3). This band is characteristic of double bonds in the planar DNA bases (*24*). From the changes in this band, it can be concluded that silica reacts with DNA and perturbs base stacking (*27*) of the DNA to some extent. This change may reflect an alteration of the secondary structure of DNA (base pairing), since spectra recorded in H_2O indicated that DNA remained in the B conformation (see above and Figure 1). Alternatively, this change may derive from bending of the DNA duplex as it wraps itself around the silica particles.

Changes in Silica Spectra after Silica–DNA Coincubation

Figure 4 shows the spectra of MQZ and MQZ + DNA (minus DNA control) between 1350 and 900 cm^{-1} in H_2O buffer. The spectrum of MQZ (Figure 4*A*) showed a major peak at 1080 cm^{-1} with a prominent shoulder peak at 1164 cm^{-1}. Corresponding peaks were seen at 1082 and 1164 cm^{-1} for CSQZ (data not shown). They are assigned to the Si–O stretching modes associated with exposure to the aqueous environment and Si–O stretching vibrations from groups inside the crystal lattice, respectively (*34,36*). Figure 5 shows the shift of the major peak in the spectrum of the dried silica film from 1063 to 1079 cm^{-1} with increasing H_2O content in the film. This confirms that the major peak at 1080 cm^{-1} in the spectrum of MQZ can be assigned to the Si–O stretch in the Si–OH group on the silica surface, with which hydrogen-bonds are formed by H_2O or DNA:

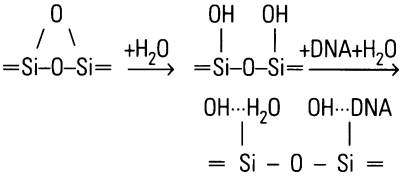

There was narrowing and shifting of the bands at 1080 cm^{-1} in the spectra of DNA + MQZ (minus DNA control) (Figure 4*B*) and DNA + CSQZ (minus DNA control) (data not shown). These

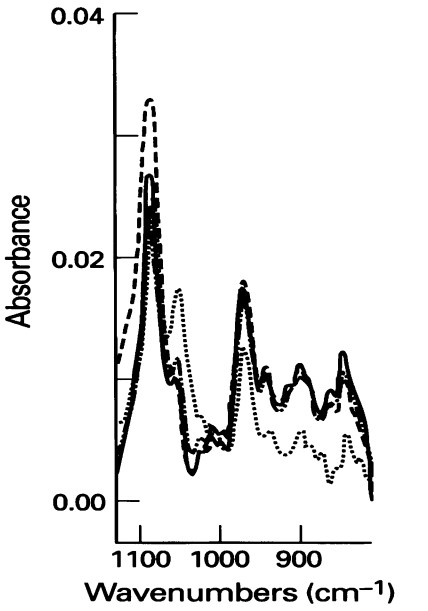

Figure 2. ATR FT-IR spectrum of calf thymus DNA (10 mg/ml in pD 7.4 phosphate-buffered D_2O) in the region 750 to 1180 cm^{-1} and the spectra of DNA coincubations with different concentrations of silica. (▪▪▪▪), DNA alone; (–▪▪–), (DNA + MQZ 0.2 mg/ml) – MQZ 0.2 mg/ml (subtraction factor is 1.025); (——), (DNA + MQZ 1.0 mg/ml) – MQZ 1.0 mg/ml (subtraction factor is 1.025); (– – – –), (DNA + MQZ 5.0 mg/ml) – MQZ 5.0 mg/ml (subtraction factor is 1.025).

changes in the spectrum may be due to the replacement of H_2O by hydrogen-bonded DNA at the Si–OH group on the silica surface.

Effect of a Surface-modifying Agent on DNA–Silica Interaction

The toxic effect of quartz on cells can be lowered markedly by pretreatment of silica with PVPNO (*32,38,39*). We therefore investigated the effect of PVPNO on the infrared spectrum of a DNA-silica mixture. The major changes induced in the bands between 1225 cm and 900 cm^{-1} of the DNA spectrum were almost completely abolished by pretreatment of quartz particles with PVPNO (Figure 6).

Discussion

This study demonstrates that DNA binds strongly to silica particles at physiologic pH. This is the first evidence of a specific binding of silica to DNA *in vitro*. The binding takes place despite the fact that the silanol and phosphate moieties involved are both acidic and thus negatively charged in an aqueous environment. Counterions, either in the buffer or as metal impurities on the silica surface, may be involved in lessening the energy barrier that must be overcome before hydrogen bonding takes place. The possible interaction of silica particles with the nuclear material inside living cells has not been investigated in the current study; cationic proteins or other molecules bound to DNA could have a similar counterion effect *in vivo*.

The observation that small silica particles may sometimes be seen by electron microscopy inside the nuclei of cultured cells (*40*) has emphasized the possibility of a direct silica–DNA interaction in cells. Such a binding, if present, could be important in the mechanisms of silica-induced disease, especially carcinogenesis. DNA bound to silica would be especially sensitive to the hydroxyl radicals produced by silica surfaces (*23*) and could suffer damage by DNA strand breakage as well as base alteration. Hydroxyl radicals, although highly damaging, are active only over distances of approximately 15 Å or one-half the diameter of a DNA helix (*41,42*). Thus DNA–silica binding could be important in bringing hydroxyl radicals close enough to cause damage to DNA, and the orientation of the binding sites may influence the type of DNA damage that takes place. In addition to hydroxyl radical mediated DNA damage, other potential effects of intracellular binding of silica to DNA might include interference with the action of DNA polymerase and physical disruption of the mitotic spindle during

Table 2. Wave numbers and intensity of bands of FT-IR spectra (800–1200cm^{-1}) of DNA and DNA + SiO_2 in buffered D_2O (10 mg/ml DNA; 1.0 mg/ml SiO_2).

DNA alone		DNA + MQZ (minus MQZ)		DNA + CSQZ (minus CSQZ)		
Wave number, cm^{-1}	Relative absorbance	Wave number, cm^{-1}	Relative absorbance	Wave number, cm^{-1}	Relative absorbance	Assignment[a]
1087	0.025	1087	0.028	1088	0.039	Sym PO_2^-
1055	0.017	1055	0.010	1052	0.005	DNA backbone
1026	0.007	1022	0.004	1022	0.005	DNA backbone
1008	0.006	1007	0.006	1008	0.007	DNA backbone
absent		988	0.005	988	0.006	DNA backbone
971	0.013	968	0.018	968	0.019	Asym O–P–O
935	0.006	938	0.010	938	0.011	DNA backbone
absent		909	0.009	909	0.010	DNA backbone
899	0.006	894	0.011	895	0.012	DNA backbone
873	0.004	absent		absent		DNA backbone
853	0.009	853	0.009	854	0.010	DNA backbone
840	0.006	839	0.012	838	0.013	DNA backbone
823	0.004	absent		absent		DNA backbone

[a]From Taillandier and Liquier (*24*) and Dev and Walters (*26*).

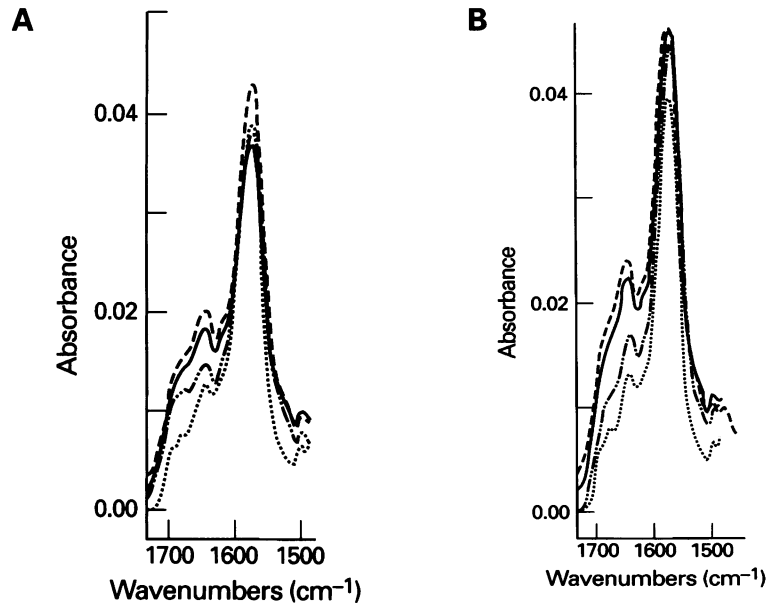

Figure 3. ATR FT-IR spectrum of calf thymus DNA (10 mg/ml in pD 7.4 phosphate-buffered D_2O) in the region 1500 to 1700 cm^{-1} and the spectra of DNA coincubations with different concentrations of silica. (*A*) (DNA + MQZ) – MQZ (subtraction factor is 1.025). (▪▪▪▪), DNA alone; (–▪▪–), (DNA + MQZ 0.2 mg/ml) – MQZ 0.2 mg/ml; (——), (DNA + MQZ 1.0 mg/ml) – MQZ 1.0 mg/ml; (– – – –), (DNA + MQZ 5.0 mg/ml) – MQZ 5.0 mg/ml. (*B*) (DNA + CSQZ) – CSQZ (subtraction factor is 1.030). (▪▪▪▪), DNA alone; (–▪▪–), (DNA + CSQZ 0.2 mg/ml) – CSQZ 0.2 mg/ml; (——), (DNA + CSQZ 1.0 mg/ml) – CSQZ 1.0 mg/ml; (– – – –), (DNA + CSQZ 5.0 mg/ml) – CSQZ 5.0 mg/ml.

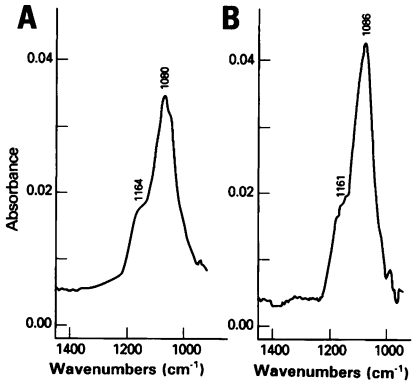

Figure 4. ATR FT-IR spectra of MQZ and (MQZ + DNA) – DNA. (*A*) MQZ alone (5 mg/ml in pH 7.4 phosphate-buffered H_2O); (*B*) (MQZ 5 mg/ml + DNA 10 mg/ml) – DNA 10 mg/ml.

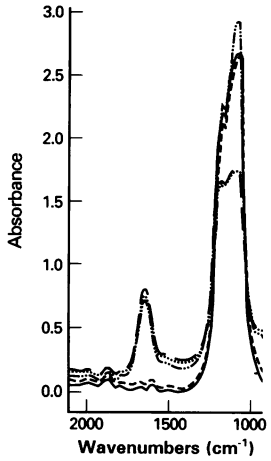

Figure 5. Transmission FT-IR spectra of the dried silica films. Only Figure 5 represents transmission FT-IR spectra; all other figures show ATR spectra. (———), dried silica film (DSF) (0.2 mg silica); (– – – –), DSF + 10 µl phosphate-buffered H_2O; (–■■–), DSF + 20 µl phosphate buffered H_2O; (■■■■), DSF + 30 µl phosphate-buffered H_2O; (— — —), DSF + 40 µl phosphate-buffered H_2O. Note: the water band at 1640 cm^{-1} is absent in the film to which 10 µl water was added because the sample did not become hydrated after addition of this small amount of water. The spectrum of the film is essentially that of the dried silica film and not indicative of partial hydration as are the other water amounts.

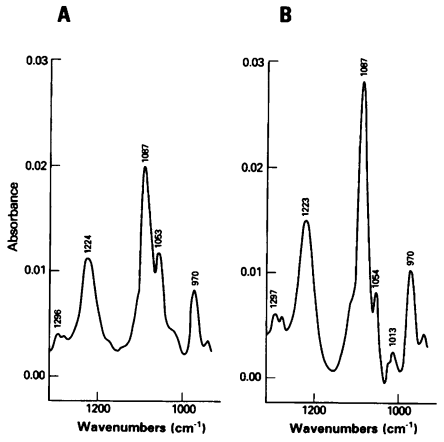

Figure 6. ATR FT-IR spectra of [(MQZ + PVPNO) + DNA] – (MQZ + PVPNO) and (MQZ + DNA) – MQZ. (*A*) –(5 mg/ml MQZ + 100 µg/ml PVPNO) + 10 mg/ml DNA – (5 mg/ml MQZ + 100 µg/ml PVPNO) (subtraction factor is 1.025); (*B*) –(5 mg/ml MQZ + 10 mg/ml DNA) – MQZ 5 mg/ml (subtraction factor is 1.025).

cell division. These could also result in genetic damage during DNA replication or repair.

DNA contains two kinds of potential nucleophilic sites which can function as hydrogen receptors: the exocyclic nitrogens or carbonyl oxygens of the purine and pyrimidine bases, and the phosphate oxygen atoms. Each of these groups is capable of forming a hydrogen bond with a hydrogen donor molecule under specific chemical conditions (*43*). The molecular vibrations arising from these different moieties of DNA are observed in specific regions of the IR spectrum.

The most meaningful changes observed in the FT-IR spectra of DNA in the silica–DNA complexes appear in the region between 1250 and 800 cm^{-1}. The shift in frequency and increase in intensity of the PO_2^- asymmetric stretch at 1225 cm^{-1} suggests that the phosphate group is an important site with which silica interacts on DNA, and is the direct target for silica binding. The intensity of the PO_2^- symmetric stretch at 1086 cm^{-1} is also increased. Although silica subtraction was normalized based on an internal standard, analysis of the changes in the latter region is more difficult due to the presence of a silica peak in this region which also changes. The observed intensity changes in the DNA spectra at 1086 cm^{-1}, cannot, however, be explained on the basis of alterations of the silica spectra used in the subtraction procedure. For example, the ATR spectrum of CSQZ (5 mg/ml) was essentially the same as that of MQZ, with an absorbance of about 0.3 at 1086 cm^{-1} (data not shown). The absorbance of DNA (10 mg/ml) in this region is 0.2 (Figure 1). These absorbances sum to 0.5, but the change in intensity at 1086 cm^{-1} in the DNA spectrum associated with CSQZ coincubation is from 0.2 to 0.65, even after subtraction of the CSQZ spectrum (Figure 1*C*). The distinct narrowing of the band width is indicative of a restriction in the mobility of this functional group and implies strong binding of the silica to DNA.

The assignment for the mode at 1053 cm^{-1} (which also shifts) is not certain. This feature has been assigned to either the PO_2^- symmetric stretching vibration (*27,28,44,45*) or to the C–O stretching vibration of the deoxyribose phosphate bond (*27,28,46,47*). We found strong absorption in the 1100 to 1000 cm^{-1} region of the FT-IR spectra by both deoxyribose and the constituent mononucleotides of DNA (AMP, CMP, GMP, TMP), using the techniques of the present study (data not shown). Thus, changes in the backbone of DNA after exposure to silica are consistent primarily with phosphate bond alteration, but some component of the nearby deoxyribose moiety cannot be excluded. In addition, some evidence exists for an as yet undefined disturbance of base pairing (as mentioned above), based on the alteration of the D_2O spectra of DNA–silica coincubations in the 1686 cm^{-1} region.

When the silica surface makes contact with water, hydration of the surface silica–oxygen bonds takes place, resulting in the formation of surface silanol groups (*48*). The silanol groups, depending on pH, are able to dissociate partially to form ionized SiO groups (*32*). Some chemicals are able to inhibit silica toxicity on cells through the modification of the silica surface (*32,38,49,50*). Covering of the silica surface silanol groups by PVPNO also effectively blocks the interaction of silica with the phosphate groups of DNA. This further supports our hypothesis that surface silanol groups are involved in the binding of silica to DNA and may be a significant factor in silica toxicity. The finding that CSQZ produces a greater alteration of the DNA spectrum than an equal weight of MQZ (Figures 1,3; Table 2) may be a consequence of the higher surface area of CSQZ (*31*), differences in surface crystal structure or differences in the level of trace surface metal impurities (*23,29*). Based on the concentrations of DNA and silica used in this study, we calculated that the ratio of surface phosphate from DNA to surface silanol from silica would be approximately 100:1 for MQZ and 29:1 for CSQZ. That observable changes in the phosphate stretching modes at 1225 and 1086 cm^{-1} do occur despite the presumably low fraction of interacting phosphate groups is remarkable, but similar results have been obtained by Theophanides (*27*), who reported changes in the FT-IR spectra of DNA induced by *cis*-platinum at phosphate to platinum ratios of 33:1. We can only speculate as to the mechanism whereby these large changes occur. They may perhaps involve a cooperative effect on the DNA helix or an overwhelmingly large effect on the phosphates which do bind.

In summary, the changes observed in the infrared spectra of DNA and silica after mixing indicate involvement of phosphate backbone and silanol groups, and suggest the formation of hydrogen bonds between the phosphate group in DNA and the silanol group on the surface of silica (Figure 7). Although the energy of each hydrogen bond is weak, the strength of the DNA–silica interaction is magnified by the additive effect of many hydrogen bonds between the polymeric DNA and crystalline silica surfaces.

Binding occurring between the phosphate backbone of DNA and the silica sur-

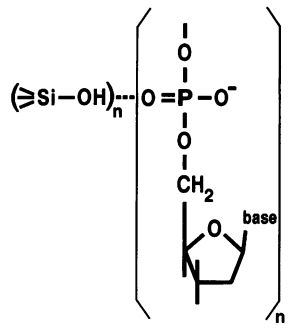

Figure 7. Proposed binding of DNA to silanol groups on the silica surface.

face may predispose DNA to strand breaks by silica through •OH. These radicals are readily produced on silica surface by direct mechanisms (*16,17,48*) or by Fenton chemistry involving trace metal (M) impurities (*23,51,52,53*):

$$H_2O_2 + M^{n+} \rightarrow \cdot OH + OH^- + M^{(n-1)+}$$

Infrared spectroscopy is a sensitive technique for the investigation of chemical interactions between silica and important biologic molecules. *In vitro* hemolysis produced by silica particles may be related to the interaction of silica with membrane proteins (*54*) and differences in the infrared spectra of silica preparations have been correlated with their hemolytic activity (*37*). Infrared spectroscopy can be useful in further elucidating the specific mechanisms of silica toxicity and in developing strategies to lessen silica toxicity by the use of modifying agents. Because each DNA molecule in the cell contains millions of phosphate groups, the potential exists for a strong interaction of DNA with silica particles internalized by the cell. We propose that such interactions represent important mechanisms of silica-induced carcinogenesis.

REFERENCES

1. Parkes WR. Occupational lung disorders. London:Butterworths, 1982;134–174.
2. Goldsmith DF, Winn DM, Shy CM, eds. Silica, Silicosis and Cancer. New York:Praeger, 1986;1–536.
3. IARC. Silica and some silicates. In: Silica and Some Silicates. IARC Monographs on the Evaluation of the Carcinogenic Risk of Chemicals to Humans, Vol 42. Lyon:International Agency for Research on Cancer, 1987;92–93.
4. Simonato L, Fletcher AC, Saracci R, Thomas TL, eds. Occupational exposure to silica and cancer risk. In: IARC Scientific Publications No 97, Lyon:International Agency for Research on Cancer, 1990;1–124.
5. Saffiotti U, Stinson SF. Lung cancer induction by crystalline silica: relationships to granulomatous reactions and host factors. Environ Carcinog Rev 6:197–122 (1988).
6. Saffiotti U. Lung cancer induction by crystalline silica. In: Relevance of Animal Studies to Evaluation of Human Cancer Risk (D'Amato R, Slaga TJ, Farland WH, Henry C, eds). New York:Wiley-Liss, 1992;51–69.
7. Spiethoff A, Wesch H, Wegener K, Klimisch HJ. The effects of thorotrast and quartz on the induction of lung tumors in rats. Health Phys 63:101–110 (1992).
8. Brown GP, Monick M, Hunninghake GW. Fibroblast proliferation induced by silica exposed human alveolar macrophages. Am Rev Respir Dis 138:85–89 (1988).
9. Miller BE, Dethloff LA, Gladen BC, Hook GER. Progression of type II cell hypertrophy and hyperplasia during silica-induced pulmonary inflammation. Lab Invest 57:546–554 (1987).
10. Lesur O, Cantin AM, Tanswell AK, Melloni B, Beaulieu JF, Bgin R. Silica exposure induces cytotoxicity and proliferative activity of type II pneumocytes. Exp Lung Res 18:173–190 (1992).
11. Hesterberg TW, Barrett JC. Dependence of asbestos- and mineral dust-induced transformation of mammalian cells in culture on fiber dimension. Cancer Res 44:2170–2180 (1984).
12. Ahmed N, Saffiotti U. Crystalline silica-induced cytotoxicity, transformation, tumorigenicity, chromosomal translocations and oncogene expression. Proc Am Assoc Cancer Res 33:119 abst (1992)
13. Nash T, Allison AC, Harington JS. Physio-chemical properties of silica in relation to its toxicity. Nature 210:259–261 (1966).
14. Bendz G, Lindqvist I, eds. Biochemistry of Silicon and Related Problems. New York:Plenum Press, 1978;3–381.
15. Shi X, Dalal NS, Hu X, Vallyathan V. The chemical properties of silica surface in relation to the silica-cell interaction in silicosis. J Toxicol Environ Health 27:435–454 (1989).
16. Karmanova EV, Myasnikov IA, Zayalov SA. Mechanism of the emission of singlet oxygen molecules from a disordered quartz surface. Zhurnal Fizichestoi Khimii 58:1958–1961 (1984).
17. Vallyathan V, Shi X, Dalal NS, Irr W, Castranova, V. Generation of free radicals from freshly fractured silica dust. Am Rev Respir Dis 138:1213–1219 (1988).
18. Fubini B, Bolis V, Giamello E, Pugliese L, Volante M. The formation of oxygen reactive radicals at the surface of the crushed quartz dusts as a possible cause of silica pathogenicity. In: Effects of Mineral Dusts on Cells (Mossman BT, Begin RO, eds). Berlin:Springer-Verlag, 1989;205–214.
19. Shi X, Dalal NS, Vallyathan V. ESR evidence for the hydroxyl radical formation in aqueous suspension of quartz particles and its possible significance to lipid peroxidation in silicosis. J Toxicol Environ Health 25:237–245 (1988).
20. Dalal NS, Shi X, Vallyathan V. Potential role of silicon-oxygen radicals in acute lung injury. NATO ASI Series H 30:265–272 (1989).
21. Doelman CJA, Leurs R, Oosterom WC, Bast A. Mineral dust exposure and free radical-mediated lung damage. Exp Lung Res 16:41–55 (1990).
22. Pairon JC, Jaurand MC, Kheuand L, Janson X, Brochard P, Bignon J. Sister chromatid exchanges in human lymphocytes treated with silica. Br J Ind Med 47:110–115 (1990).
23. Daniel LN, Mao Y, Saffiotti U. Oxidative DNA damage by crystalline silica. Free Radic Biol Med 14:463–472 (1993).
24. Taillandier E, Liquier J. Infrared spectroscopy of DNA. Methods Enzymol 211:307–335 (1992).
25. Harris PI, Chapman D. Does Fourier-transform infrared spectroscopy provide useful information on protein structure? Trends Biochem Sci 17:328–333 (1992).
26. Dev SB, Walters L. Fourier transform infrared spectroscopy for the characterization of a model peptide-DNA interaction. Biopolymers 29:289–299 (1990).
27. Theophanides T. Fourier transform infrared spectra of calf thymus DNA its reactions with the anticancer drug cisplatin. Appl Spectrosc 35:461–465 (1981).
28. Keller PB, Hartman KA. The effect of ionic environment and mercury (II) on the alternative structures of DNA. An infrared spectroscopic study. Spectrochimica Acta 42A:299–306 (1986).
29. Fu SC, Yang GC, Shong MZ, Du QZ. Characterization of a new standard quartz and its effects in animals [in Chinese]. Chinese J Indust Hyg Occup Dis 2:134–137 (1984).
30. Brunauer S, Emmett PH, Teller E. Adsorption of gases in multimolecular layers. J Am Chem Soc 60:309–319 (1938).
31. Daniel LN, Mao Y, Vallyathan V, Saffiotti U. Binding of the cationic dye, Janus green B, as a measure of the specific surface area of crystalline silica in aqueous suspension. Toxicol Appl Pharmacol 123:62–67 (1993).
32. Nolan RP, Langer AM, Harrington JS, Oster G, Selikoff, IJ.

Quartz hemolysis as related to its surface functionalities. Environ Res 26:503–520 (1981).
33. Covington AR, Paabo M, Robinson RA, Bates RG. Use of the glass electrode in deuterium oxide and the relation between the standardized pD (paD) scale and the operational pH in heavy water. Anal Chem 40:700–706 (1968).
34. Willis HA, Van der Mass JH, Miller RGJ, eds. Laboratory Methods in Vibrational Spectroscopy. New York:John Wiley and Sons, 1987;430–432.
35. Dev SB, Keller J, Rha CK. Secondary structure of 11 S globulin in aqueous solution investigated by FT-IR derivative spectroscopy. Biochim Biophys Acta 957:272–280 (1988).
36. Mohr SC, Sokolov NVHA, He C, Setlow P. Binding of small acid-soluble spore proteins from Bacillus subtilis changes the conformation of DNA from B to A. Proc Natl Acad Sci USA 88:77–81 (1991).
37. Pandurangi S, Seehra MS, Razzaboni BL, Bolsaitis P. Surface and bulk infrared modes of crystalline and amorphous silica particles: a study of the relation of surface structure to cytotoxicity of respirable silica. Environ Health Perspect 86:327–336 (1990).
38. Klockars M, Hedenborg M, Vanhala E. Effect of two particle surface-modifying agents, polyvinylpyridine-*N*-oxide and carboxymethylellulose, on the quartz and asbestos mineral fiber-induced production of reactive oxygen metabolites by human polymorphonuclear leukocytes. Arch Environ Health 45:8–14 (1990).
39. Nyberg P. Polyvinylpyridine-*N*-oxide and carboxymethyl cellulose inhibit mineral dust-induced production of reactive oxygen species by human macrophages. Environ Res 55:157–164 (1991).
40. Saffiotti U, Daniel LN, Mao Y, Williams AO, Kaighn ME, Ahmed N, Knapton AD. Biological studies on the carcinogenic mechanisms of quartz. Rev Mineralogy 28:523–544 (1993).
41. Ward JE, Blakely WF, Jones EI. Mammalian cells are not killed by DNA single-strand breaks caused by hydroxyl radicals from hydrogen peroxide. Radiat Res 103:383–392 (1985).
42. Meneghini R. Genotoxicity of active oxygen species in mammalian cells. Mut Res 195:215–230 (1988).
43. Ruddon RW. Chemical mutagenesis. In: Principles of Drug Action: The Basis of Pharmacology (Pratt WB, Taylor P, eds). New York:Churchill Livingstone, 1990;691–733.
44. Sutherland GBBM, Tsuboi M. The infrared spectrum and molecular configuration of sodium deoxyribonucleate. Proc R Soc Lond (Math Phys) A239:446–463 (1957).
45. Manfait M, Theophanides T. Fourier transform infrared spectra of cells treated with drug adriamycin. Biochem Biophys Res Commun 116:321–326 (1983).
46. Tsuboi M. Application of infrared spectroscopy to structure studies of nucleic acids. In: Applied Spectroscopy Reviews, Vol 3 (Brame EG, ed). New York:Dekker, 1969;45–90.
47. Taillandier E, Liquier J, Taboury J, Ghomi M. Structure transitions in DNA (A,B,Z) studied by IR spectroscopy. In: Spectroscopy of Biological Molecules (Sandorfy C, Theophanides T, eds). Boston:Reidel, 1984;171–189.
48. Hochstrasser G, Antonini JF. Surface states of pristine silica surfaces. Surface Sci 32:644–664 (1972).
49. Wiessner JH, Mandel NS, Sohnle PG, Hasegawa A, Mandel GS. The effect of chemical modification of quartz surfaces on particulate-induced pulmonary inflammation and fibrosis in the mouse. Am Rev Respir Dis 141:111–116 (1990).
50. Vallyathan V, Kang JH, Van dyke K, Dalal NS, Castranova V. Response of alveolar macrophages to *in vitro* exposure to freshly fractured versus aged silica dust: the ability of prosil 28, an organosilane material, to coat silica and reduce its biological reactivity. J Toxicol Environ Health 33:303–315 (1991).
51. Kennedy TP, Dodson R, Rao NV, Ky H, Hopkins C, Baser M, Tolley E, Hoidal JR. Dusts causing pneumoconiosis generate •OH and produce hemolysis by acting as Fenton catalysts. Arch Biochem Biophys 269:359–364 (1989).
52. Ghio AJ, Kennedy TP, Whorton AR, Crumbliss, AL, Hatch GE, Hoidal JR. Role of surface complexed iron in oxidant generation and lung inflammation induced by silicates. Am J Physiol 263:L511–L518 (1992).
53. Ghio AJ, Hatch GE. Lavage phosphlipid concentration after silica instillation in the rat is associated with complexed (Fe^{3+}) on the dust surface. Am J Respir Cell Mol Biol 8:403–407 (1993).
54. Summerton J, Hoenig S, Butler C, Chvapil M. The mechanism of hemolysis by silica and its bearing on silicosis. Exp Mol Path 26:113–118 (1977).